Characterization and Application of Nanomaterials (2023) Volume 6 Issue 2
doi:10.24294/can.v6i2.3314

ORIGINAL RESEARCH ARTICLE

Cross-linked polymer nanocomposite networks coated nano sand light-weight proppants for hydraulic fracturing applications

Mohan Raj Krishnan[1,*], Wengang Li[2,*], Edreese Housni Alsharaeh[1,*]

[1] *College of Science and General Studies, Alfaisal University, PO Box 50927, Riyadh, 11533, Saudi Arabia.*

[2] *EXPEC Advanced Research Center, Saudi Aramco, PO Box 5000, Dhahran, 31311, Saudi Arabia.*

*** Corresponding authors:** Mohan Raj Krishnan, mkrishnan@alfaisal.edu; Wengang Li, wengag.li@aramco.com; Edreese Housni Alsharaeh, ealsaraeh@alfaisal.edu

ABSTRACT

Three-dimensionally cross-linked polymer nanocomposite networks coated nano sand light-weight proppants (LWPs) were successfully prepared via ball-milling the macro sand and subsequently modifying the resultant nano sand with sequential polymer nanocomposite coating. The modified nano sand proppants had good sphericity and roundness. Thermal analyses showed that the samples can withstand up to 411 °C. Moreover, the proppant samples' specific gravity (S.G.) was 1.02–1.10 g/cm^3 with excellent water dispersibility. Therefore, cross-linked polymer nanocomposite networks coated nano sand particles can act as potential candidates as water-carrying proppants for hydraulic fracturing operations.

Keywords: proppants; nano sand; polymer; nanocomposites; graphene; hydraulic fracturing

ARTICLE INFO

Received: 16 November 2023
Accepted: 22 November 2023
Available online: 29 November 2023

1. Introduction

In general, proppants are milli- or micrometer-sized solid particles with specific crush resistance employed to keep open the cracks and enhance oil production from a wellbore[1–5]. Since the proppants are used in downhole a few kilometers deep, they must be stable at harsh conditions of high temperature and high pressure (HT-HP), high temperature-high salinity (HT-HS) coming from either groundwater in deep wells or the strong acid mixtures (hydrofluoric and hydrochloric acids) that are pumped into wellbore to clear blockages, and corrosion from the fracturing fluid itself[1,6–22]. Therefore, the nature and quality of the proppant are vital to a successful hydraulic fracturing operation and subsequent oil production. Frac sand and modified frac sands are widely employed as proppants[23–26]. Even though the frac is abundantly available and has a low cost due to its high density, low crush resistance (6000 psi), and relatively decreased sphericity and roundness, it often causes poor fracture permeability[2,27,28]. Conversely, although the ceramic proppants have very high crush resistance (up to 20,000 psi) and thermal stability, the settling rate in fracturing fluid is high, which is ascribed to their high specific gravity values (3 g/cm^3)[2,28–33]. Hence, various conventional hydraulic fracturing operations exploit large volumes of water-based hydraulic fluid to enhance the well permeability, potentially producing large amounts of wastewater as flow back and pose severe environmental threats[33–39]. Therefore, water-based fracturing technology has recently attracted the attention of scientists, and it

requires the development of ultra-lightweight proppant[40–44]. At the same time, the ultra-lightweight proppants should possess excellent crush resistance, thermal stability, acid resistance, and higher roundness and sphericity.

Polymeric composite microspheres have been recently employed as low-density proppants for water-based hydraulic fracturing operations[4,42,44–47]. For instance, Chen et al.[48] reported polymethylmethacrylate (PMMA)/graphite composite microspheres with SG of 1.055–1.135 g/cm^3 and can withstand crushing stress up to 69 MPa. They have also reported polystyrene (PS)/graphite microspheres with SG of 1.025–1.185 g/cm^3 with a crush resistance of 68 MPa[49]. The primary preparation methods of the polymeric microspheres are emulsion polymerization, suspension polymerization, dispersion polymerization, and so on[50–52]. However, this method involves multi-step syntheses with yield limitations and is most often not scalable to meet the growing industrial demands[53–64]. Therefore, we conceived the idea of making nano sand particles by ball-milling the abundant and low-cost frac sand and suitably modifying them to withstand high temperature-high pressure-high salinity (HT-HP-HS) downhole conditions[17]. Incorporating nanofillers like graphene can potentially increase the final material's thermal and mechanical properties[65,66]. To our knowledge, no publications exist on nano sand particles as lightweight proppants in hydraulic fracturing applications. We have recently reported different surface modification techniques using various polymers, resins, and their combinations to improve the crush resistance of frac sand. The existing modification techniques are majorly of one-layer coating, and there is still space for improvement in thermo-mechanical and structural integrities in the coated sand proppants[45,67]. Our group has recently introduced a two-layer coating approach for the surface modification of frac sand using sequential coating polymer nanocomposites with graphene or boron nitride nanosheets. Interestingly, the two-layer coating sand proppants exhibited a crush resistance to a maximum of 10,000-14,000 psi[2,28,33,68–70]. However, practical applications of these proppants are limited due to their high specific gravity values and poor dispersibility in water-based fracturing fluid. Also, pumping the high-density proppants into formations may result in discontinuous structures that may have an adverse impact on oil production. Therefore, the proppants with ultra-low density, good water dispersibility (low-settling rate), and enhanced thermal properties are highly preferred.

In this study, we aimed to fabricate cross-linked polymer nanocomposite networks modified nano sand particles as a potential proppant candidate for successful hydraulic fracturing. In addition, the present study also reports the successful co-polymerization of styrene (S), methyl methacrylate (MMA), and divinylbenzene (DVB) into a cross-linked nanonetwork onto the nano sand particles. The first-layer modified nano sand particles were further subjected to another modification using an epoxy-CG (commercial graphene) composite layer. In contrast to the conventional resin coating approaches, this method applies a direct co-polymerization onto the nano sand surfaces and subsequent second-layer modification. In an alternative approach, nano sand particles were pre-modified with zirconia nanoparticles (ZrO_2) as an attempt to enhance the inter-layer interaction of an inorganic component (nano sand surface) to a polymer layer (organic component). The nano sand-based lightweight proppants with reinforced thermo-mechanical properties and high crush resistance can be potential water-carrying fracturing proppants. The novelty of the work is the utilization of nano sand derived from the abundant natural source of macro sand through ball-milling and its successful surface modification with a two-layer polymer composite layer.

2. Experimental

2.1. Chemicals

The monomers styrene with a purity of >99% (S), methyl methacrylate with a purity of 99% (MMA), and divinylbenzene with a purity of >99% (MMA) were purchased from Sigma Aldrich. The monomers were used as received. Azoisobutyronitrile (AIBN) was obtained from Aldrich and recrystallized using methanol. Saudi Aramco provided us with sand samples, epoxy resin, and the curing agent. The commercial graphene (CG)

was procured from XG Sciences. ZrO_2 samples were prepared in our laboratory[15].

2.2. Preparation of nano sand and ZrO_2 modified nano sand

Nano sand samples were prepared by ball milling the frac sand particles for 12 h. To prepare the ZrO_2-modified nano sand, the nano sand sample is mixed with a specific amount of ZrO_2 nanoparticles and ball-milled for another hour. The experimental preparation for ZrO_2 can be found elsewhere[14,15].

2.3. Preparation of dual-coated nano sand proppants

A sequential coating of cross-linked PS-PMMA/DVB nanonetworks (layer 1) and epoxy-CG composite (layer 2) onto the nano sand surface was used to prepare lightweight nano sand proppants. The cross-linked PS-PMMA/DVB nanonetworks onto nano sand particle surfaces were prepared by carrying out an in-situ cross-linking and one-step copolymerization of S and MMA monomers (1:1 wt%), with DVB (10 wt% to S: MMA mixture) as a cross-linker with AIBN as an initiator (0.01 wt% to the monomer and cross-linker mixture). To carry out the surface polymerization, the monomer, cross-linker, and initiator mixture (5 wt% to the nano sand weight) is well-mixed with nano sand samples and heated to 70 °C. Cross-linked co-polymer networks' modified nano sand was mixed with 4:1 wt% of epoxy resin, curing agent, and CG (0.001 wt% to epoxy resin) and treated at 150 °C for curing of the epoxy. The curing reaction is optimized to be 5 min. The PS-PMMA coating on the nano sand was carried out using the same procedure but without adding the DVB.

2.4. Characterizations

2.4.1. X-ray diffraction (XRD)

The Rigaku MiniFlex 600 instrument was used to record the XRD patterns for the samples. The diffraction measurements were recorded in the range of 5°–80°.

2.4.2. Thermal analysis

Thermogravimetric analyses (TGA, Hitachi STA7200) evaluated the samples' degradation temperatures (T_{deg}). The measurements were conducted from 30 °C to 500 °C at a heating rate of 10 °C/min under a constant inert gas (N_2) flow.

3. Results and discussion

3.1. Preparation of cross-linked PS-PMMA/DVB nanonetworks and Epoxy-CG nanocomposite modified nano sand particles

Figure 1 shows a sequential two-layer coating of cross-linked PS-PMMA/DVB layer followed by an Epoxy-CG layer onto nano sand surfaces. The first layer of cross-linked PS-PMMA/DVB nanonetworks onto the surface of nano sand was prepared by polymerizing monomers mixture of S and MMA, cross-linker DVB, with the aid of AIBN at 70 °C. The detailed formation and the mechanistic pathway for the cross-linked PS-PMMA/DVB nanonetworks can be found in our previous reports[2,28,33,68,70]. At 70 °C, the AIBN produces free radicals, and the monomers are converted into free radicals instantaneously. Then, the monomer radicals reacted randomly with other monomers, and the polymeric chain propagated. At the same time, the growing polymer chains also randomly reacted with the DVB molecules, resulting in the cross-linking of polymer chains[2,39,71]. Therefore, a cross-linked PS-PMMA/DVB nanonetwork is formed on the surface of the nano sand. The second layer of Epoxy-CG was prepared using an epoxy resin, curing agent, and CG that was cured at 150 °C for 5 min.

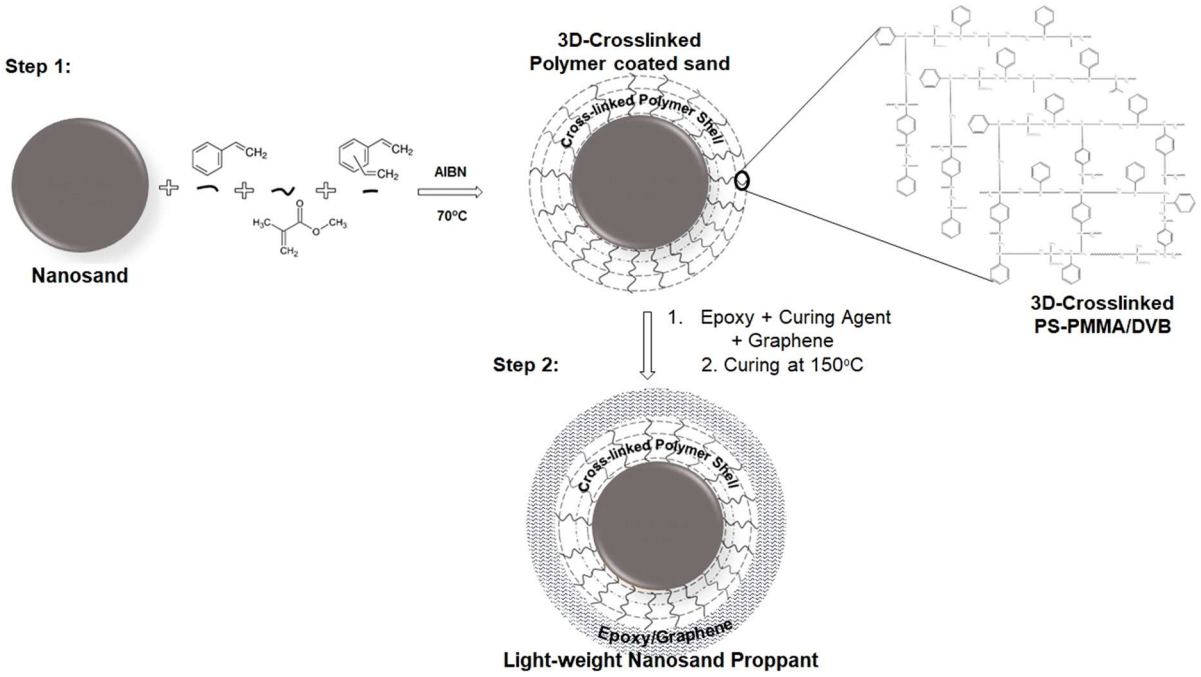

Figure 1. Sequential two-layer coating of cross-linked PS-PMMA/DVB layer followed by Epoxy-CG layer onto nano sand surfaces.

3.2. XRD

Figure 2 shows the XRD of micro sand (100 mesh) and nano sand samples that were prepared by ball-milling for various times ranging from 1 to 12 h. The peaks detected at 21°, 26.5°, 42°, 44°, 51°, 58°, 68°, 77° are assigned to SiO_2 (quartz phase). As for the micro sand, two major peaks were observed: one is at 21° (100), and the other is at 26.5°. When the micro sand is subjected to ball-milling for 1 h, the intensities of 100 and 101 peaks are slightly reduced. The decrease in the peak intensities is more evident when the ball-milling time is increased, for instance, from 2 h to 12 h. The reduction in the intensities of the characteristic peaks of frac sand can directly be related to the particle size of the resultant ball-milled nano sand particles. Using Debye-Scherer's equation, the particle sizes can be calculated for each hour of ball-milling. The nano sand's average particle size was 9 nm for the sample ball-milled for 12 h.

Figure 3 shows the XRD for the nano sand (ball-milled for 12 h), epoxy-CG (commercial graphene) composite coating layer, and modified nano sand with one- or two-layer polymer composite coating layers with and without ZrO_2 cross-linker modification of the nano sand. As for the nano sand, the characteristic peaks detected at 21°, 26.5°, 42°, 44°, 51°, 58°, 68°, and 77° correspond to the quartz phase of SiO_2. For the epoxy-CG, peaks were detected at 15°, 18°, and 26° and attributed to CG; for the samples of NS-(Epoxy-CG), NS-(PS-PMMA-CG-ZrO_2)-(Epoxy-CG), NS-(PS-PMMA-ZrO_2-CG)-(Epoxy-CG), NS-ZrO_2-(PS-PMMA)-(Epoxy-CG), NS-ZrO_2-(PS-PMMA-CG-ZrO_2)-(Epoxy-CG), and NS-ZrO_2-(PS-PMMA)-(Epoxy-CG), the characteristic peak position and their relative intensities of the nano sand were not altered. This indicates that the relative weight ratio of the coating layers to nano sand particles is low enough as the peak position or the intensities are unchanged.

Figure 4 shows the XRD patterns for the nano sand modified with epoxy-CG, NS-(PS-PMMA)-(Epoxy-CG), NS-(PS-PMMA-CG)-(Epoxy-CG), NS-(PS-PMMA/DVB)-(Epoxy-CG), and NS-(PS-PMMA/DVB-CG)-(Epoxy-CG). As evident from the unaltered the characteristic peak position and intensities of the nano sand weight ratio of the nano sand to coating layers particles are much lower.

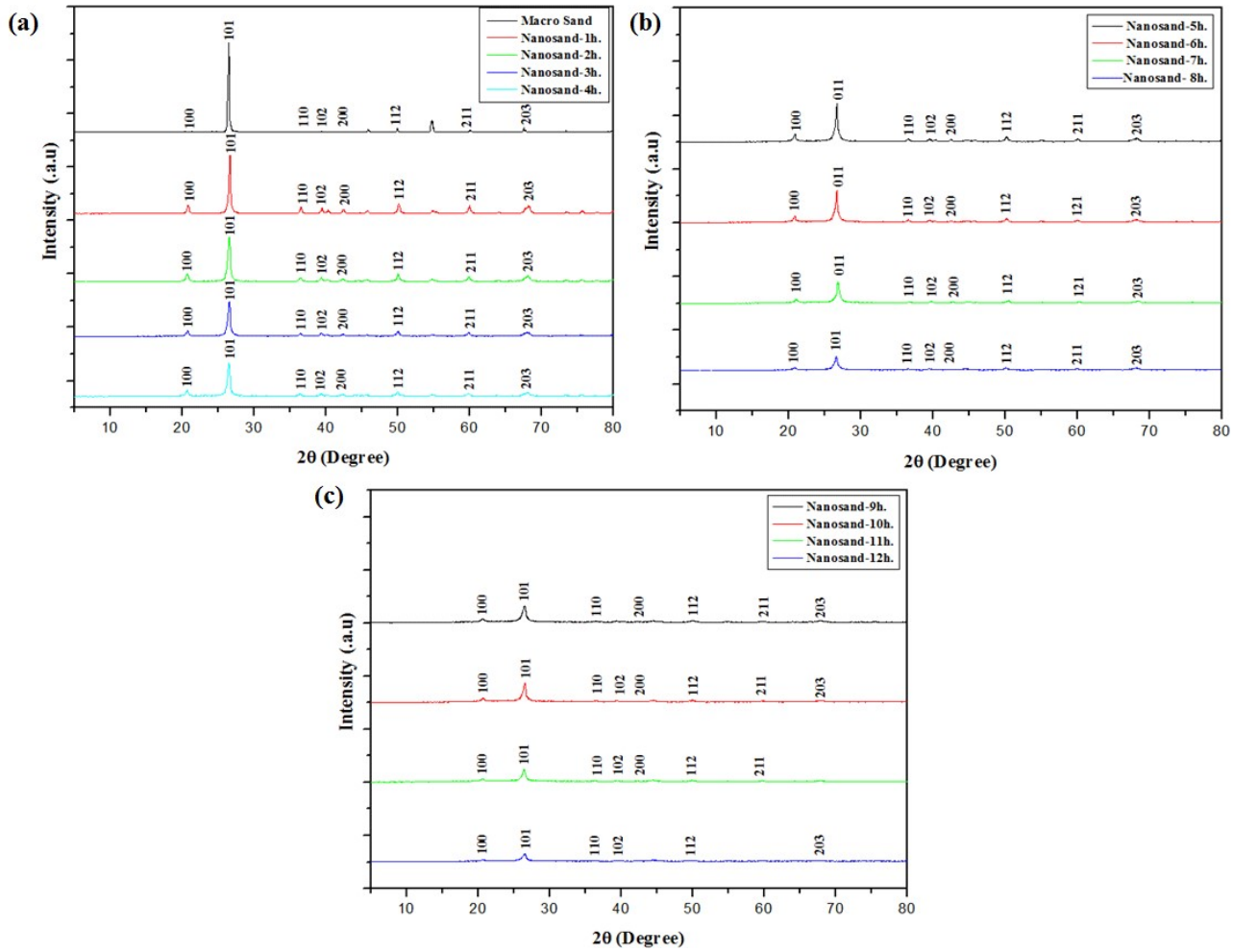

Figure 2. XRD of Ball-milled sand samples for 0–12 h. **(a)** 0–4 h, **(b)** 5–8 h, and **(c)** 9–12 h.

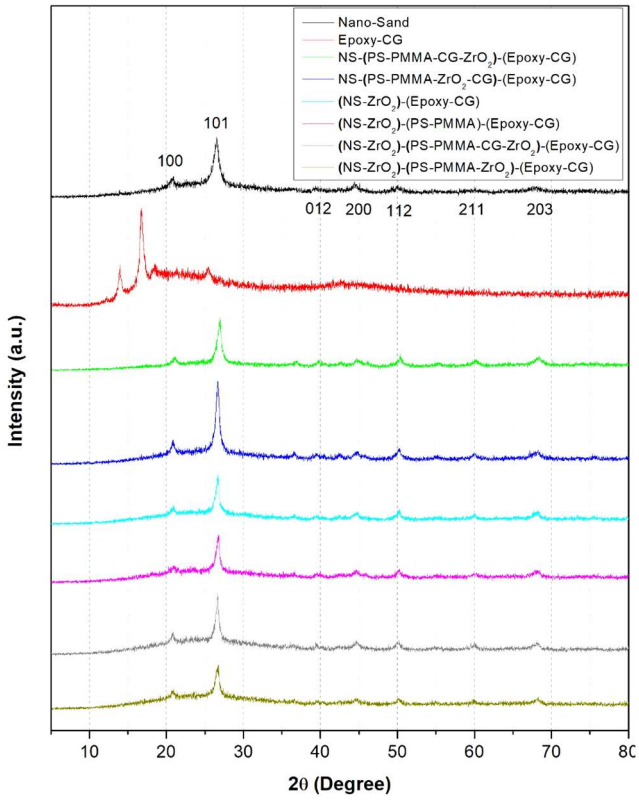

Figure 3. XRD patterns of coated nano sand proppants with ZrO_2 as a cross-linker in comparison to neat nano sand and epoxy-CG.

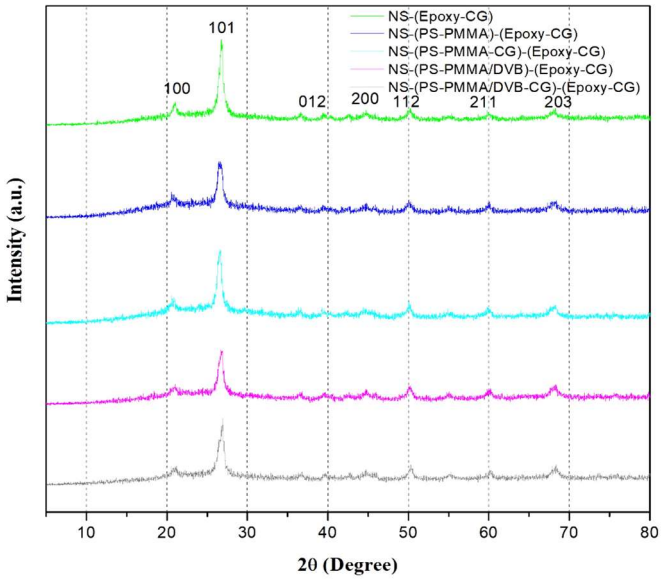

Figure 4. XRD patterns of coated nano sand proppants with DVB as a cross-linker.

3.3. Thermal stability analyses

Thermal degradation temperatures (T_{deg}) of the modified nano sand proppant samples were evaluated using their respective TGA curves. **Figure 5** shows the TGA of neat-nano sand, epoxy-CG, nano sand-(ZrO_2)-(Epoxy-CG), nano sand-(ZrO_2)-(PS-PMMA)-(Epoxy-CG), nano sand-(ZrO_2)-(PS-PMMA-ZrO_2)-(Epoxy-CG), nano sand-(ZrO_2)-(PS-PMMA-CG)-(Epoxy-CG), nano sand-(ZrO_2)-(PS-PMMA-CG-ZrO_2)-(Epoxy-CG), and nano sand-(PS-PMMA-CG-ZrO_2)-(Epoxy-CG). The T_{deg} was calculated using a differential thermal curve for the samples with clear degradation steps. However, for the samples with no clear degradation patterns, the temperature at which half of the weight loss was observed was considered to be their T_{deg}[72]. The nano sand lost weight at 500 °C, while the epoxy-CG layer had a degradation peak at 362 °C. When the ZrO_2-modified nano sand is coated with an epoxy-CG layer, the T_{deg} is increased to 365 °C, and this thermal stability enhancement is a clear indication of cross-linking of ZrO_2 to the epoxy layer. For the samples of nano sand-(ZrO_2)-(PS-PMMA)-(Epoxy-CG), nano sand-(ZrO_2)-(PS-PMMA-ZrO_2)-(Epoxy-CG), nano sand-(ZrO_2)-

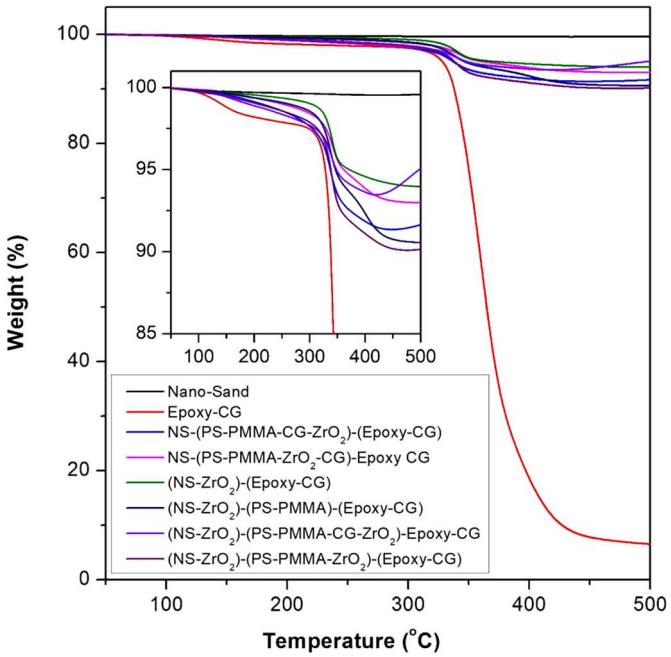

Figure 5. TGA of coated nano sand proppants with ZrO_2 as a cross-linker compared to neat nano sand and epoxy-CG. Inset: Magnified plot.

(PS-PMMA-CG)-(Epoxy-CG), nano sand-(ZrO_2)-(PS-PMMA-CG-ZrO_2)-(Epoxy-CG), T_{deg} values are 368 ℃, 369 ℃, 371 ℃, and 371 ℃, respectively. From these results, it can be noted that polymer and polymer composite coating of PS-PMMA and PS-PMMA-CG, in addition to the epoxy-CG coating onto the ZrO_2-modified nano sand, would further enhance the stabilities of the respective proppant samples. Interestingly, for the sample of nano sand-(PS-PMMA-CG- ZrO_2)-(Epoxy-CG), the T_{deg} value is 375 ℃. This can be attributed to the higher cross-linking ability of ZrO_2 between PS-PMMA-CG and epoxy-CG layers. Therefore, it is more desirable to have cross-linked dual-coating of copolymer-2D nanofiller composite and cured resin composite onto nano sand particles for the successful hydraulic fracture operation with modified nano sand as proppants.

Figure 6 shows the TGS curves for nano sand-(PS-PMMA)-(Epoxy-CG), nano sand-(PS-PMMA-CG)-(Epoxy-CG), nano sand-(PS-PMMA/DVB)-(Epoxy-CG), and nano sand-(PS-PMMA/DVB-CG)-(Epoxy-CG) in comparison to nano sand-(Epoxy-CG) and neat-nano sand. **Table 1** summarizes all the degradation temperatures of the samples. As shown in **Figure 6**, the T_{deg} values are found to be 372 ℃, 375 ℃, 396 ℃, and 411 ℃ for nano sand-(PS-PMMA)-(Epoxy-CG), nano sand-(PS-PMMA-CG)-(Epoxy-CG), nano sand-(PS-PMMA/DVB)-(Epoxy-CG), and nano sand-(PS-PMMA/DVB-CG)-(Epoxy-CG) respectively. This increase can be explained by forming 3D- nanonetworks of PS-PMMA/DVB. This can be credited to the higher thermal stability of the epoxy-CG composite layer. Interestingly, a synergistic increase in the degradation temperature values for the samples with a two-layer coating of cross-linked PS-PMMA/DVB followed by Epoxy-CG coating was observed. Therefore, these proppant samples would be highly suitable for high-temperature wells.

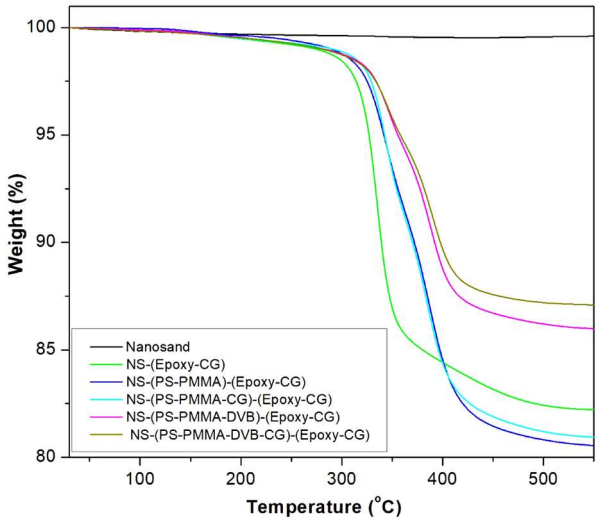

Figure 6. Compared to neat nano sand and epoxy-CG, TGA curves for coated nano sand proppants with DVB as a cross-linker.

Table 1. Summary of thermal properties of the nano sand-based proppants.

Sample	T_{deg} (℃)	SG (g/cm^3)
Nano sand	-	1.02
Epoxy-CG	362	-
Nano sand-(**ZrO_2**)-(Epoxy-CG)	365	1.05
Nano sand-(**ZrO_2**)-(PS-PMMA)-(Epoxy-CG)	368	1.07
Nano sand-(**ZrO_2**)-(PS-PMMA-**ZrO_2**)-(Epoxy-CG)	369	1.09
Nano sand-(**ZrO_2**)-(PS-PMMA-CG)-(Epoxy-CG)	371	1.08
Nano sand-(**ZrO_2**)-(PS-PMMA-CG-**ZrO_2**)-(Epoxy-CG)	372	1.10
Nano sand-(PS-PMMA-CG-**ZrO_2**)-(Epoxy-CG)	375	1.08
Nano sand-(Epoxy-CG)	336	1.04
Nano sand-(PS-PMMA)-(Epoxy-CG)	372	1.06
Nano sand-(PS-PMMA-CG)-(Epoxy-CG)	375	1.07
Nano sand-(PS-PMMA/DVB)-(Epoxy-CG)	396	1.07
Nano sand-(PS-PMMA/DVB-CG)-(Epoxy-CG)	411	1.09

3.4. Specific gravity (SG) and water suspension analyses

The specific gravity of the nano sand proppant samples was summarized in **Table 1**. The neat-nano sand has an SG value as low as 1.02. At the same time, the SG values for nano sand-(ZrO_2)-(Epoxy-CG), nano sand-(ZrO_2)-(PS-PMMA)-(Epoxy-CG), nano sand-(ZrO_2)-(PS-PMMA-ZrO_2)-(Epoxy-CG), nano sand-(ZrO_2)-(PS-PMMA-CG)-(Epoxy-CG), nano sand-(ZrO_2)-(PS-PMMA-CG-ZrO_2)-(Epoxy-CG), nano sand-(PS-PMMA-CG- ZrO_2)-(Epoxy-CG), and nano sand-(PS-PMMA-CG-ZrO_2)-(Epoxy-CG) are 1.05, 1.07, 1.09, 1.08, 1.08 and 1.10. The values indicate that the SG values also increase when we increase the coating layer and materials. Similarly, for the samples of nano sand-(PS-PMMA)-(Epoxy-CG), nano sand-(PS-PMMA-CG)-(Epoxy-CG), nano sand-(PS-PMMA/DVB)-(Epoxy-CG), and nano sand-(PS-PMMA/DVB-CG)-(Epoxy-CG), the S.G values are found to be 1.06, 1.07, 1.07, and 1.09. The values indicate that the SG values also increase when we increase the coating layer and the coating materials.

Figure 7 shows the suspension of the nano sand proppant samples of nano sand-(PS-PMMA/DVB)-(Epoxy-CG) and nano sand-(PS-PMMA-ZrO_2)-(Epoxy-CG) in gulf sea water after 1 h of dispersion in comparison neat-nano sand and correspondingly modified macro sand sample. It can be seen that the macro sand proppant particles are instantaneously settled in the water, whereas the neat nano sand remains suspended because of its low SG value of 1.02. For the modified nano sand proppant samples, the one with (PS-PMMA/DVB)-(Epoxy-CG) suspended in the seawater for a longer time in comparison to the one with (PS-PMMA-ZrO_2)-(Epoxy-CG). This observation is consistent with their corresponding SG values.

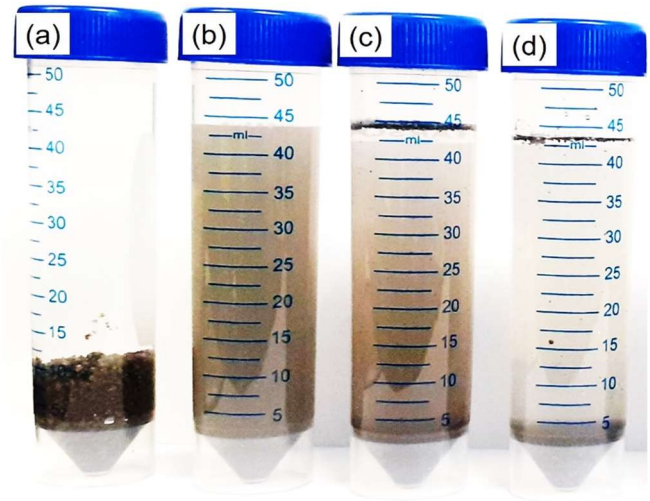

Figure 7. Suspension of coated nano sand lightweight proppants compared to coated macro sand proppants after 1 h of dispersion in Gulf Sea water. **(a)** Coated macro sand[2,28], **(b)** neat-nano sand, **(c)** nano sand-(PS-PMMA/DVB)-(Epoxy-CG), and **(d)** nano sand-(PS-PMMA-ZrO_2)-(Epoxy-CG).

Besides, the S.G. of the nano sand-(PS-PMMA/DVB)-(Epoxy-CG) proppant is determined to be only 1.09 g/cm^3 while that of resin-coated sand proppant counterparts is 1.40g/cm^3. The decrease in bulk density of the developed nano sand-(PS-PMMA/DVB)-(Epoxy-CG) proppants is an obvious indication of successful dual coating of cross-linked polymer nanonetworks and epoxy-graphene composite layer while not compromising the permeability of the fractures.

4. Conclusion

Two-layer coated nano sand particles were successfully prepared via ball-milling the macro sand and subsequently modifying the resultant nano sand with polymer nanocomposites with different surface modifications. The first layer of cross-linked PS-PMMA/DVB was prepared using S and MMA monomers, crosslinker (DVB) at 70 °C. The second layer of Epoxy-CG was prepared using a mixture of Epoxy resin, a

curing agent, and CG that was cured at 150 °C for 5 min. XRD and TGA studies confirmed successful surface coatings onto the nano sand particles. The dual-coating layer of (PS-PMMA/DVB)-(Epoxy-CG) exhibited thermal stability up to 411 °C. Nevertheless, specific gravity (SG) analysis illustrated that the density of the proppants was about 1.02–1.10 g/cm^3 with good dispersion in water. Thermal studies showed that the samples can withstand up to 411 °C. Therefore, the polymer nanocomposite-modified nano sand proppant samples can act as potential candidates as water-carrying proppants in oil and gas industries. The thermally enhanced polymer nanocomposites modified nano sand proppant samples with low S.G. values and excellent water dispersibility characteristics would be highly useful for the current oil and gas industries.

Author contributions

Conceptualization, MRK, WL, and EHA; methodology, MRK; validation, WL and EHA; formal analysis, WL; investigation, MRK; resources, WL; data curation, MRK and EHA; writing—original draft preparation, MRK; writing—review and editing, MRK, WL, and EHA; supervision, WL and EHA; project administration, MRK; funding acquisition, WL and EHA. All authors have read and agreed to the published version of the manuscript.

Acknowledgments

This study is part of research project agreement no. AFU-01-2017 in collaboration with EXPEC Advanced Research Centre, Saudi Aramco. The authors gratefully acknowledge the continued support from AlFaisal University and its Office of Research.

Conflict of interest

The authors report that there is no conflict of interest to declare.

References

1. Gao W, He S, Jie J. Evaluation on long-term flow conductivity of coated proppants (Chinese). *Natural Gas Industry* 2007; 27(10): 100–102.
2. Krishnan MR, Aldawsari Y, Michael FM, et al. Mechanically reinforced polystyrene-polymethyl methacrylate copolymer-graphene and Epoxy-Graphene composites dual-coated sand proppants for hydraulic fracture operations. *Journal of Petroleum Science and Engineering* 2021; 196: 107744. doi: 10.1016/j.petrol.2020.107744
3. Liang F, Sayed M, Al-Muntasheri GA, et al. A comprehensive review on proppant technologies. *Petroleum* 2016; 2(1): 26–39. doi: 10.1016/j.petlm.2015.11.001
4. Michael FM, Krishnan MR, Li W, Alsharaeh EH. A review on polymer-nanofiller composites in developing coated sand proppants for hydraulic fracturing. *Journal of Natural Gas Science and Engineering* 2020; 83: 103553. doi: 10.1016/j.jngse.2020.103553
5. Raysoni N, Weaver JD. Long-term proppant performance. In: SPE International Symposium and Exhibition on Formation Damage Control; February 15–17 2012; Lafayette, Louisiana, USA. doi: 10.2118/150669-MS
6. Belyadi H, Fathi E, Belyadi F. Proppant characteristics and application design. In: Belyadi H, Fathi E, Belyadi F (editors). *Hydraulic Fracturing in Unconventional Reservoirs*. Gulf Professional Publishing; 2017. pp. 73–96. doi: 10.1016/B978-0-12-849871-2.00006-X
7. Howard GC, Fast CR. *Hydraulic Fracturing*. Society of Petroleum Engineers; 1970. 210p.
8. Mader D. In: Mader D (editor). *Hydraulic Proppant Fracturing and Gravel Packing*. 1st ed. Elsevier Science; 1989.
9. Montgomery CT, Smith MB. Hydraulic fracturing: History of an enduring technology. *Journal of Petroleum Technology* 2010; 62(12): 26–40. doi: 10.2118/1210-0026-JPT
10. Nguyen PD, Weaver JD, Dewprashad BT, et al. Enhancing fracture conductivity through surface modification of proppant. In: SPE Formation Damage Control Conference; 18–19 February 1998; Lafayette, Louisiana, USA. doi: 10.2118/39428-MS
11. Norman LR, Terracina JM, McCabe MA, Nguyen PD. Application of curable resin-coated proppants. *SPE Production & Operation* 1992; 7(4): 343–349. doi: 10.2118/20640-PA
12. Salah M, El-Sebaee M, Batmaz T. Channel fracturing technology: A paradigm shift in stimulation of tight reservoir and unlock production potential. In: SPE Europec Featured at 79th EAGE Conference and Exhibition; 12–15 June

2017; Paris, France. doi: 10.2118/185873-MS
13. Wu T, Wu B, Zhao S. Acid resistance of silicon-free ceramic proppant. *Materials Letters* 2013; 92: 210–212. doi: 10.1016/j.matlet.2012.10.124
14. Michael FM, Krishnan MR, AlSoughayer S, et al. Thermo-elastic and self-healing polyacrylamide -2D nanofiller composite hydrogels for water shutoff treatment. *Journal of Petroleum Science and Engineering* 2020; 193: 107391. doi: 10.1016/j.petrol.2020.107391
15. Michael FM, Krishnan MR, Fathima A, et al. Zirconia/graphene nanocomposites effect on the enhancement of thermo-mechanical stability of polymer hydrogels. *Materials Today Communications* 2019; 21: 100701. doi: 10.1016/j.mtcomm.2019.100701
16. Almohsin A, Michal F, Alsharaeh E, et al. Self-healing PAM composite hydrogel for water shutoff at high temperatures: Thermal and rheological investigations. In: SPE Gas & Oil Technology Showcase and Conference; 21–23 October 2019; Dubai, UAE. doi: 10.2118/198664-MS
17. Almohsin A, Alsharaeh E, Michael FM, Krishnan MR. Polymer-Nanofiller Hydrogels. U.S. Patent 20,220,290,033A1, 15 September 2022.
18. Almohsin A, Alsharaeh E, Krishnan MR. Polymer-Sand Nanocomposite Lost Circulation Material. U.S. Patent 20,230,142,223A1, 11 May 2023.
19. Almohsin AM, Alsharaeh E, Krishnan MR, Alghazali M. Coated Nanosand as Relative Permeability Modifier. U.S. Patent 20,230,060,690A1, 2 March 2023.
20. Almohsin A, Krishnan MR, Alsharaeh E, Harbi B. Preparation and properties investigation on sand-polyacrylamide composites with engineered interfaces for water shutoff applications. In: Middle East Oil, Gas and Geosciences Show; 19–21 February 2023; Manama, Bahrain. doi: 10.2118/213481-MS
21. Krishnan MR, Li W, Alsharaeh EH. Ultra-lightweight nanosand/polymer nanocomposite materials for hydraulic fracturing operations. *SSRN e-Journal* 2022. doi: 10.2139/ssrn.4233321
22. Krishnan M, Michal F, Alsoughayer S, et al. Thermodynamic and kinetic investigation of water absorption by PAM composite hydrogel. In: SPE Kuwait Oil & Gas Show and Conference; 13–16 October 2019; Mishref, Kuwait. doi: 10.2118/198033-MS
23. Fu L, Zhang G, Ge J, et al. Surface modified proppants used for porppant flowback control in hydraulic fracturing. *Colloids and Surfaces A: Physicochemical and Engineering Aspects* 2016; 507: 18–25. doi: 10.1016/j.colsurfa.2016.07.039
24. Liu P, Guo S, Lian M, et al. Improving water-injection performance of quartz sand proppant by surface modification with surface-modified nanosilica. *Colloids and Surfaces A: Physicochemical and Engineering Aspects* 2015; 470: 114–119. doi: 10.1016/j.colsurfa.2015.01.073
25. Qian T, Muhsan A, Htwe L, et al. Urethane based nanocomposite coated proppants for improved crush resistance during hydraulic fracturing. *IOP Conference Series: Materials Science and Engineering* 2020; 863: 012013. doi: 10.1088/1757-899X/863/1/012013
26. Tabatabaei M, Dahi Taleghani A, Cai Y, et al. Using nanoparticles coating to enhance proppant functions to achieve sustainable production. In: SPE Annual Technical Conference and Exhibition; 30 September–2 October 2019; Calgary, Alberta, Canada. doi: 10.2118/196067-MS
27. Bestaoui-Spurr N. Materials science improves silica sand strength. In: SPE International Symposium and Exhibition on Formation Damage Control; 26–28 February 2014; Lafayette, Louisiana, USA. doi: 10.2118/168158-MS
28. Krishnan MR, Aldawsari Y, Michael FM, et al. 3D-Polystyrene-polymethyl methacrylate/divinyl benzene networks-Epoxy-Graphene nanocomposites dual-coated sand as high strength proppants for hydraulic fracture operations. *Journal of Natural Gas Science and Engineering* 2021; 88: 103790. doi. 10.1016/j.jngse.2020.103790
29. Biryukova A, Dzhienalyev T, Panichkin A. Ceramic proppants for hydraulic fracturing. *IOP Conference Series: Materials Science and Engineering* 2021; 1040: 012008. doi. 10.1088/1757-899X/1040/1/012008
30. Hao J, Ma H, Feng X, et al. Microstructure and fracture mechanism of low density ceramic proppants. *Materials Letters* 2018; 213: 92–94. doi. 10.1016/j.matlet.2017.11.021
31. Liang F, Sayed M, Al-Muntasheri G, Chang FF. Overview of existing proppant technologies and challenges. In: SPE Middle East Oil & Gas Show and Conference; 8–11 March 2015; Manama, Bahrain. doi: 10.2118/172763-MS
32. Man S, Wong RCK. Compression and crushing behavior of ceramic proppants and sand under high stresses. *Journal of Petroleum Science and Engineering* 2017; 158: 268–283. doi: 10.1016/j.petrol.2017.08.052
33. Krishnan MR, Omar H, Aldawsari Y, et al. Insight into thermo-mechanical enhancement of polymer nanocomposites coated microsand proppants for hydraulic fracturing. *Heliyon* 2022; 8(12): e12282. doi: 10.1016/j.heliyon.2022.e12282
34. Aramendiz J, Imqam A. Water-based drilling fluid formulation using silica and graphene nanoparticles for unconventional shale applications. *Journal of Petroleum Science and Engineering* 2019; 179: 742–749. doi: 10.1016/j.petrol.2019.04.085
35. Parizad A, Shahbazi K, Ayatizadeh Tanha A. Enhancement of polymeric water-based drilling fluid properties using nanoparticles. *Journal of Petroleum Science and Engineering* 2018; 170: 813–828. doi:

10.1016/j.petrol.2018.06.081
36. Krishnan MR, Alsharaeh E. Potential removal of benzene-toluene-xylene toxic vapors by nanoporous poly(styrene-r-methylmethacrylate) copolymer composites. *Environmental Nanotechnology, Monitoring & Management* 2023; 20: 100860. doi: 10.1016/j.enmm.2023.100860
37. Krishnan MR, Omar H, Almohsin A, Alsharaeh EH. An overview on nanosilica–polymer composites as high-performance functional materials in oil fields. *Polymer Bulletin* 2023. doi: 10.1007/s00289-023-04934-y
38. Krishnan MR, Aldawsari YF, Alsharaeh EH. Three-dimensionally cross-linked styrene-methyl methacrylate-divinyl benzene terpolymer networks for organic solvents and crude oil absorption. *Journal of Applied Polymer Science* 2021; 138(9): 49942. doi: 10.1002/app.49942
39. Krishnan MR, Aldawsari YF, Alsharaeh EH. 3D-poly(styrene-methyl methacrylate)/divinyl benzene-2D-nanosheet composite networks for organic solvents and crude oil spill cleanup. *Polymer Bulletin* 2021; 79: 3779–3802. doi: 10.1007/s00289-021-03565-5
40. Boyou NV, Ismail I, Sulaiman WRW, et al. Experimental investigation of hole cleaning in directional drilling by using nano-enhanced water-based drilling fluids. *Journal of Petroleum Science and Engineering* 2019; 176: 220–231. doi: 10.1016/j.petrol.2019.01.063
41. Cheraghian G, Wu Q, Mostofi M, et al. Effect of a novel clay/silica nanocomposite on water-based drilling fluids: Improvements in rheological and filtration properties. *Colloids and Surfaces A: Physicochemical and Engineering Aspects* 2018; 555: 339–350. doi: 10.1016/j.colsurfa.2018.06.072
42. Feng Y-C, Ma C-Y, Deng J-G, et al. A comprehensive review of ultralow-weight proppant technology. *Petroleum Science* 2021; 18: 807–826. doi: 10.1007/s12182-021-00559-w
43. Kulkarni MC, Ochoa OO. Mechanics of light weight proppants: A discrete approach. *Composites Science and Technology* 2012; 72(8): 879–885. doi: 10.1016/j.compscitech.2012.02.017
44. Tasqué JE, Vega IN, Marco S, et al. Ultra-light weight proppant: Synthesis, characterization, and performance of new proppants. *Journal of Natural Gas Science and Engineering* 2021; 85: 103717. doi: 10.1016/j.jngse.2020.103717
45. Danso DK, Negash BM, Ahmed TY, et al. Recent advances in multifunctional proppant technology and increased well output with micro and nano proppants. *Journal of Petroleum Science and Engineering* 2021; 196: 108026. doi: 10.1016/j.petrol.2020.108026
46. Pangilinan KD, de Leon ACC, Advincula RC. Polymers for proppants used in hydraulic fracturing. *Journal of Petroleum Science and Engineering* 2016; 145: 154–160. doi: 10.1016/j.petrol.2016.03.022
47. Zoveidavianpoor M, Gharibi A. Application of polymers for coating of proppant in hydraulic fracturing of subterraneous formations: A comprehensive review. *Journal of Natural Gas Science and Engineering* 2015; 24: 197–209. doi: 10.1016/j.jngse.2015.03.024
48. Chen T, Wang Y, Yan C, et al. Preparation of heat resisting poly(methyl methacrylate)/graphite composite microspheres used as ultra-lightweight proppants. *Journal of Applied Polymer Science* 2015;132(18): 41924. doi: 10.1002/app.41924
49. Han X, Cheng Q, Bao F, et al. Synthesis of low-density heat-resisting polystyrene/graphite composite microspheres used as water carrying fracturing proppants. *Polymer-Plastics Technology and Engineering* 2014; 53(16): 1647–1653. doi: 10.1080/03602559.2014.919648
50. Brooks B. Suspension polymerization processes. *Chemical Engineering & Technology* 2010; 33(11): 1737–1744. doi: 10.1002/ceat.201000210
51. Kawaguchi S, Ito K. Dispersion polymerization. In: Okubo M (editor). *Polymer Particles*. Springer Berlin, Heidelberg; 2005. pp. 299–328. doi: 10.1007/b100118
52. Wang Q, Fu S, Yu T. Emulsion polymerization. *Progress in Polymer Science* 1994; 19(4): 703–753. doi: 10.1016/0079-6700(94)90031-0
53. Samitsu S, Zhang R, Peng X, et al. Flash freezing route to mesoporous polymer nanofibre networks. *Nature Communications* 2013; 4: 2653. doi: 10.1038/ncomms3653
54. Krishnan MR, Samitsu S, Fujii Y, Ichinose I. Hydrophilic polymer nanofibre networks for rapid removal of aromatic compounds from water. Chemical Communications 2014; 50(66): 9393–9396. doi: 10.1039/C4CC01786B
55. Krishnan MR, Chien YC, Cheng CF, Ho RM. Fabrication of mesoporous polystyrene films with controlled porosity and pore size by solvent annealing for templated syntheses. *Langmuir* 2017; 33(34): 8428–8435. doi: 10.1021/acs.langmuir.7b02195
56. Krishnan MR, Lu K-Y, Chiu W-Y, et al. Directed self-assembly of star-block copolymers by topographic nanopatterns through nucleation and growth mechanism. *Small* 2018; 14(16): 1704005. doi: 10.1002/smll.201704005
57. Lo T-Y, Krishnan MR, Lu K-Y, Ho R-M. Silicon-containing block copolymers for lithographic applications. *Progress in Polymer Science* 2018; 77: 19–68. doi: 10.1016/j.progpolymsci.2017.10.002
58. Cheng C-F, Chen Y-M, Zou F, et al. Li-ion capacitor integrated with nano-network-structured Ni/NiO/C anode and nitrogen-doped carbonized metal–organic framework cathode with high power and long cyclability. *ACS Applied Materials & Interfaces* 2019; 11(34): 30694–30702. doi: 10.1021/acsami.9b06354

59. Chien Y-C, Huang L-Y, Yang K-C, et al. Fabrication of metallic nanonetworks via templated electroless plating as hydrogenation catalyst. *Emergent Materials* 2021; 4: 493–501. doi: 10.1007/s42247-020-00108-y
60. Krishnan MR, Almohsin A, Alsharaeh EH. Syntheses and fabrication of mesoporous styrene-co-methyl methacrylate-graphene composites for oil removal. *Diamond and Related Materials* 2022; 130: 109494. doi: 10.1016/j.diamond.2022.109494
61. Krishnan M, Chen H-Y, Ho R-M. Switchable structural colors from mesoporous polystyrene films. *Abstracts of papers–American Chemical Society* 2016.
62. Bongu CS, Krishnan MR, Soliman A, et al. Flexible and freestanding MoS_2/Graphene composite for high-performance supercapacitors. *ACS Omega* 2023; 8(40): 36789–3680. doi: 10.1021/acsomega.3c03370
63. Krishnan MR, Rajendran V, Alsharaeh E. Anti-reflective and high-transmittance optical films based on nanoporous silicon dioxide fabricated from templated synthesis. *Journal of Non-Crystalline Solids* 2023; 606: 122198. doi: 10.1016/j.jnoncrysol.2023.122198
64. Krishnan MR, Alsharaeh EH. Polymer gel amended sandy soil with enhanced water storage and extended release capabilities for sustainable desert agriculture. *Journal of Polymer Science and Engineering* 2023; 6(1): 2892. doi: 10.24294/jpse.v6i1.2892
65. Jbur AQ, Abdullah WN, Faleh NM, Faleh ZN. Vibration analysis of graphene platelet reinforced stadium architectural roof shells subjected to large deflection. *Structural Engineering and Mechanics* 2023; 86(2): 157–165. doi: 10.12989/sem.2023.86.2.157
66. Al-Jaafari MAA, Ahmed RA, Fenjan RM, Faleh NM. Nonlinear dynamic characteristic of sandwich graphene platelet reinforced plates with square honeycomb core. *Steel and Composite Structures* 2023; 46(5): 659–667. doi: 10.12989/scs.2023.46.5.659
67. Guo T, Wang Y, Du Z, et al. Evaluation of coated proppant unconventional performance. *Energy & Fuels* 2021; 35(11): 9268–9277. doi: 10.1021/acs.energyfuels.1c00187
68. Li W, Alsharaeh E, Krishnan MR. Coated Proppant and Methods of Making and Use Thereof. U.S. Patent 20,230,313,027A1, 5 October 2023.
69. Li W, Alsharaeh E, Krishnan MR. Proppant coatings and methods of making. U.S. Patent 20,210,395,603A1, 23 December 2021.
70. Li W, Alsharaeh E, Krishnan MR. Methods for Making Proppant Coatings. U.S. Patent 11,459,503, 4 October 2022.
71. Krishnan MR, Aldawsari YF, Alsharaeh EH. Three-dimensionally cross-linked styrene-methyl methacrylate-divinyl benzene terpolymer networks for organic solvents and crude oil absorption. *Journal of Applied Polymer Science* 2021; 138(9): 49942. doi: 10.1002/app.49942
72. Tiwari A, Hihara LH. Thermal stability and thermokinetics studies on silicone ceramer coatings: Part 1-inert atmosphere parameters. *Polymer Degradation and Stability* 2009; 94(10): 1754–1771. doi: 10.1016/j.polymdegradstab.2009.06.010